ACVR2A Facilitates Trophoblast Cell Invasion through TCF7/c-JUN Pathway in Pre-eclampsia Progression

Shujing Yang[1#], Huanyao Liu[1#], Jieshi Hu[1], Bingjun Chen[1], Wanlu An[1], Xuwen Song[1], Yi Yang[1*], Fang He[1*]

[1]Department of Obstetrics and Gynecology, Obstetrics; Guangdong Provincial Key Laboratory of Major Obstetric Diseases; Guangdong Provincial Clinical Research Center for Obstetrics and Gynecology; Guangdong-Hong Kong-Macao Greater Bay Area Higher Education Joint Laboratory of Maternal-Fetal Medicine; The Third Affiliated Hospital, Guangzhou Medical University, Guangzhou, China.

[#]These authors contributed equally: Shujing Yang, Huanyao Liu

*email: Yangyi@gzhmu.edu.cn ; hefangjnu@126.com

Abstract

Pre-eclampsia (PE) is a serious pregnancy disorder linked to genetic factors, particularly the ACVR2A gene, which encodes a receptor involved in the activin signaling pathway and plays a critical role in reproductive processes. Transcriptomic data analysis and experimental verification confirmed a downregulation of ACVR2A expression in placental tissues from PE patients. In this study, CRISPR/Cas9 technology was employed to investigate the effect of ACVR2A gene deletion on trophoblast cells using the HTR8/SVneo and JAR cell lines.. Deletion of ACVR2A inhibits trophoblastic migration, proliferation, and invasion, underscoring its pivotal role in cellular function. RNA-seq data analysis unveiled an intricate regulatory

network influenced by ACVR2A gene knockout, especially in the TCF7/c-JUN pathway. By employing RT-PCR and immunohistochemical analysis, a potential association between ACVR2A and the TCF7/c-JUN pathway was hypothesized and confirmed. The complexity of PE onset and the significance of genetic factors were emphasized, particularly the role of the ACVR2A gene identified in GWAS. This study established a robust foundation for delving deeper into the intricate mechanisms of PE, paving the way for focused early intervention, personalized treatment, and enhanced obstetric healthcare.

Keywords: Pre-eclampsia, ACVR2A, HTR8/SVneo, JAR, TCF7, c-JUN

INTRODUCTION

Pre-eclampsia (PE) is a pregnancy-related disorder characterized by hypertension and proteinuria typically occurring after the 20th week of gestation [1]. The clinical manifestations of PE range from asymptomatic high blood pressure detected during routine prenatal examinations to severe symptoms such as seizures, respiratory distress, upper abdominal discomfort, and evident placental abruption [2]. Genetic factors play a crucial role in PE, with a positive family history being a significant risk factor. The pathogenesis and mechanisms underlying PE remain unclear, with suggested mechanisms including endothelial damage, excessive immune activation, nutritional deficiencies, genetic factors, and insulin resistance [3, 4]. The inadequate infiltration of trophoblasts leading to impaired remodeling of uterine spiral arteries is believed to be a key factor in the development of PE. Additionally, immune responses, abnormal

renin-angiotensin system activity, inflammation, and platelet activation are implicated in the pathogenesis of PE. Investigating the interplay and mechanisms of these factors is crucial for understanding and addressing the occurrence and progression of PE [2].

Genome-Wide Association Studies (GWASs) have significantly advanced the understanding of the genetic basis of various common diseases over the past decade, including those related to pregnancy complications such as PE. By examining single nucleotide polymorphisms (SNPs) across millions of genetic loci in thousands of individuals, GWASs can identify genetic markers associated with an increased risk of a disease [5]. In the context of PE, GWASs has facilitated the identification of multiple risk loci related to biological processes such as vascular formation, blood pressure regulation, and immune response [6]. Despite these advancements, the genetic structure of PE is complex, and the effect of a single genetic variation is generally modest. Consequently, functional studies are often necessary to interpret GWAS results and elucidate specific pathological mechanisms.

Recent research in the field of PE GWASs has highlighted the pivotal role of the ACVR2A gene, particularly in the development of hypertensive disorders of pregnancy (HDP) and PE [7]. Studies conducted in various populations, including the Philippines, Northeast Brazil, Australia/New Zealand, Norway, and China, consistently demonstrated significant associations between ACVR2A gene polymorphisms and PE susceptibility [8-15]. ACVR2A, located on chromosome 2q22, is a critical member of the receptor family mediating activin function within the transforming growth factor-β (TGF-β) ligand family, exerting diverse biological functions [16]. Increased activin A

concentrations, primarily originating from the placenta, have been notably observed in the development of HDP. ACVR2A's effect extends to promoting endometrial decidualization and playing an essential role in the growth and development of the placenta and embryo [17]. As a receptor for activin A, ACVR2A is indispensable in regulating reproductive functions such as decidualization, trophoblast invasion, and placental formation during pregnancy [15]. The receptor's predominant expression in the endometrium, placenta, and vascular endothelial cells underscores its core role in pregnancy-related mechanisms [18]. Collectively, these findings support the hypothesis that ACVR2A gene polymorphisms may disrupt placental formation, contributing to early-onset PE. Taken together, these findings substantiate the hypothesis that polymorphisms in the ACVR2A gene could impede placental formation, thereby contributing to the early onset of PE.

MATERIALS AND METHODS

Collection of Placenta and Decidua Specimens/Subject Recruitment and Placental Sampling

This study was approved by the Hospital Ethics Committee (SWYX:NO2021-352). 10 PE patients and 10 normal pregnancy patients admitted to the Third Affiliated Hospital of Guangzhou Medical University for cesarean section from October 2022, to October 2023, were randomly selected. The exclusion criteria included gestational diabetes, cardiovascular disease, history of thyroid disease, history of autoimmune disease, history of hypertension, intrahepatic cholestasis of pregnancy, anemia,

infectious disease, drug use, recent acute or chronic infectious disease, and incomplete information recording. The control group consisted of 10 non-hypertensive healthy pregnant women who underwent cesarean section due to breech and cicatricial uterus. In accordance with the guidelines from the American College of Obstetricians and Gynecologists, PE is diagnosed in patients with a systolic blood pressure of 140 mm Hg or more, a diastolic blood pressure of 90 mm Hg or more, or both. Table S1 summarizes the clinical characteristics of the study population.

All specimens were collected during cesarean section. Within 5 minutes after delivery of the placenta, the placental tissue was cut vertically at the junction between the center of the placenta and the umbilical cord, the size of which was about 1 × 1 × 1 cm, and the obvious abnormal parts, such as placental bleeding, infarction, and calcification, were avoided. The placental tissue was repeatedly rinsed with sterile saline to remove blood, cut into fragments under sterile conditions, and immediately placed in a cryogenic tube and frozen in liquid nitrogen. Then, it was transferred to a refrigerator at −80 °C within 24 h.

Cell Line

The human HTR8/SVneo trophoblast cell line was purchased from the U.S. Typical Culture Preservation Center. The human placental villus cancer cell JAR was purchased from Wuhan Punosei Life Technology Co., Ltd. No other cell contamination was identified by STR. A mycoplasma test kit (Servicebio, China) was used every 2 weeks to test for mycoplasma to ensure that the cell was negative. The cells were cultured with RPMI 1640 medium (Gibco) containing 10% fetal bovine serum (FBS,

Gibco) and 1% penicillin/streptomycin (Servicebio, China) and placed in a constant temperature incubator at 37 °C and 5% CO_2.

CRISPR/Cas9-targeted Deletion of ACVR2A

ACVR2A sgRNAs were designed in the provided web tool (https://portals.broadinstitute.org/gppx/crispick/public). Two guide RNA (sgRNA) sequences were chosen (forward: 5′-GAA GGC ACA TCC TGA CTT GT-′; reverse: 5′-GAT GAC ACA ATCTTCTGCAC-3′). Subsequently, the selected sgRNAs were assessed for potential off-target sites by using the following website: http://www.rgenome.net/cas-offinder/. The sgRNAs were synthesized separately by in-vitro transcription, and each was combined with a gRNA-scaffold to from the final sgRNA. The sgRNAs were then combined with the Cas9 protein to form a ribonucleoprotein (RNP) complex. This RNP complex was introduced into the HTR8/SVneo and JAR cell lines using electroporation. Specifically, electroporation was performed using the Celetrix, following the manufacturer's protocol with the sgRNA-Cas9 mixed solution and buffer solution OPTI-MEM. After electroporation, the cells were cultured in RPMI 1640 medium with 10% FBS for 24 hours. Successful incorporation of the RNP complex was confirmed by PCR and sequencing. The confirmation of ACVR2A deletion in single monoclonal cell lines involved a multistep validation process, including Sanger sequencing, agarose gel electrophoresis and RT-PCR. Primers specifically designed for ACVR2A gene knockout verification were used in the validation process (Table S4).

RT-qPCR

For RNA extraction, cDNA reverse transcription cell RNA was isolated using a total RNA separation kit (TIANGEN, China) in accordance with the manufacturer's instructions as described above. The primers were synthesized by Takara (Japan), and the sequence of primers is shown in Table S2. The mRNA levels were quantified by SYBR Green (Roche, Germany), and dissolution curve analysis was performed to ensure amplification specificity. A total of 40 PCR cycles were performed in a Bio-Rad CFX Connect real-time system. The initial enzyme activation and template were as follows: denatured at 95 °C for 10 min and then at 95 °C for 5 s, annealed at 63.3 °C for 30 s, and extended at 72 °C for 10 s. Subsequently, the dissolution curves were analyzed. Period threshold (Ct) values were used for quantification. The efficiency values for all tests ranged from 95% to 100%.

Western Blot Analysis

Cells were harvested using a cell scraper and resuspended in RIPA buffer supplemented with a protease inhibitor cocktail and a phosphatase inhibitor (Sigma–Aldrich, USA). The cell suspension was then incubated on ice for 30 min to ensure complete lysis. After incubation, the lysates were centrifuged at 12,000 rpm for 15 minutes at 4 °C to remove cell debris. The supernatant containing the protein lysates was collected, and the protein concentration was determined using the BCA protein assay kit (Thermo Fisher Scientific, USA). For tissue samples, placental tissues were homogenized in RIPA buffer with the same supplements (protease and phosphatase inhibitors). The homogenate was incubated on ice for 30 minutes and then centrifuged at 12,000 rpm for 15 minutes at 4°C to remove debris. The supernatant containing the

protein lysates was collected, and protein concentration was similarly determined using the BCA protein assay kit. Subsequently, equal amounts of protein samples were separated through SDS-PAGE and electro-transferred onto a PVDF membrane (EMD Millipore, Germany). The membrane was then subjected to blocking with 5% BSA in TBST (TBS, pH 7.4, 0.2% Tween-20) and incubated overnight at 4 °C with primary antibodies targeting ACVR2A (Thermo Fisher Scientific, USA) and GAPDH (Santa Cruz, USA). On the next day, the membrane was thoroughly washed three times with TBST, followed by incubation with Dylight 680-conjugated secondary antibodies (KPL, USA) in darkness for 2 h. All membrane images were captured using a Li-Cor Odyssey Clx Infrared Imaging System (LI-Cor Biotechnology, Lincoln, NE, USA), and densitometry analysis of bands was conducted utilizing ImageJ software.

IHC Staining and Data Analysis

IHC staining was conducted on 4 μm paraffin sections, which were dried for 30 min at 60 °C, followed by dewaxing using an environmentally friendly solution and gradual dehydration through an alcohol gradient. Subsequently, antigen retrieval was performed at 98 °C in EDTA with a pH of 9.0 for 15 min, and endogenous peroxidase activity was quenched with 3% H_2O_2 at room temperature for 25 min. The sections were incubated overnight at 4 °C with an appropriate antibody concentration (the corresponding item number and diluted concentration of antibody are shown in Table S4). Following PBS washing, the sections were subjected to 50 min incubation with HRP-labeled secondary antibodies at room temperature. The immunoperoxidase signal was visualized using a 3,3′-diaminobenzene solution, followed by hematoxylin

counterstaining. The IHC staining was evaluated at 400× magnification and scored by two independent pathologists. Finally, quantification was performed using ImageJ, and statistical analysis was conducted using a t-test.

CCK-8 Assay for Cell Proliferation

The WT cells (WT group) and ACVR2A-knockout cells (ACVR2A-KO group) were seeded in 96-well plates at a density of 10,000 cells per well and incubated overnight in 100 μL medium. Cell proliferation was evaluated using CCK-8 assay (CAT: G4103-1ML, Servicebio) in accordance with the manufacturer's instructions. The CCK-8 reagent was applied to the cells at 24, 48, and 72 h. After the cells were incubated at 37 °C for 2 h, the optical density of the samples was measured at a wavelength of 450 nm by using a microplate reader, and the cell growth curve was generated.

Wound Healing Assay

The capacity of ACVR2A to enhance migration in JAR and HTR8/SVneo cells was assessed through wound healing (scratch) assays. The cell lines were seeded into six-well culture plates and allowed to reach 90% confluence. A sterile 200 μL pipette tip was employed to generate a singular wound/scratch on the cellular monolayer. The detached surface cell debris was removed by rinsing with PBS, and 1640 medium supplemented with 1% FBS was introduced to each well. Cellular images were captured at 0, 24, 48, and 72 h by using a phase contrast microscope. The migratory capability of the cells was determined at 24, 48, and 72 h post-scratch by measuring the width of the wound in three randomly selected fields simultaneously. The migration index was

computed using the following formula, with T representing time (24, 48, or 72 h):

$$\text{Healing Rate}(\%) = \left(\frac{\text{0H scratch area} - \text{TH scratch area}}{\text{0H scratch area}}\right) \times 100\%$$

The data shown represent the mean and standard deviation (SD) of three independent experiments.

Transwell invasion assays

First, the upper chamber of the Transwell insert was coated with Matrigel and allowed to gelate at 37 °C. Next, 15×10^4 cells from each cell line were suspended in a serum-free medium. They were inoculated on a 12-well Transwell insert with a pore size of 8 μm (Corning, USA). Next, 800 μL of growth medium was added to the lower chamber, which was then incubated at 37 °C for 24 h. Afterwards, the cells in the chamber are carefully removed. The migrating cells at the base of the Transwell insert were fixed with 4% paraformaldehyde (PFA) and stained with 1% crystal violet. Next, the invading cells were captured using a 100× optical microscope, and the cells were counted at five different 300× fields of view.

Plate Cloning Formation Assay

Colony formation assays were conducted using ACVR2A knockout JAR and HTR8/SVneo cell lines. For each group, the cells were seeded at a density of 1000 cells/well in a six-well plate (NEST) containing 15% fetal bovine serum supplemented with 1640 medium and cultured for 14 days. The medium was changed every 3 days. When the majority of cell clones expanded to more than 100 cells, the cells were washed with PBS, fixed with 4% PFA for 20 min, and stained with 1% crystal violet for 20 min at room temperature. The excess crystal violet was washed away with PBS,

and the dishes were air dried. The cell clones were manually counted under a dissecting microscope. The statistical data on colony formation were derived from three independent experiments and expressed as mean ± SD.

Transcriptomic Analysis

RNA was meticulously extracted from four distinct cell lines (ACVR2A KO-JAR and WT-JAR, ACVR2A KO-HTR8/SVneo and WT-HTR8/SVneo) by utilizing the TRIzol reagent, strictly adhering to the manufacturer's guidelines (Invitrogen, USA). NanoDrop 2000 (Thermo Fisher Scientific, USA) and the RNA Nano 6000 Assay Kit (derived from the Agilent Bioanalyzer 2100 system, Agilent Technologies, CA, USA) were employed to ensure the pristine quality of the pre-sequencing of the RNA samples. These measures served to comprehensively assess the purity, concentration, and integrity of the RNA samples. The subsequent transcriptomic analysis was adeptly executed by Biomker Technologies (Guangzhou, China).

The DESeq2 R package (version 1.10.1) was used for meticulous exploration of differential expression within the two groups. Rigorous statistical adjustments were applied to the resulting p-values by using Benjamini and Hochberg's method, effectively controlling the false discovery rate (FDR). Conforming to the DESeq2 criteria, genes with an adjusted p-value < 0.05 were precisely delineated as differentially expressed. The differential expression profiles of these samples were further dissected using the EBSeq R package. The posterior probability of being differentially expressed was harnessed to refine the resultant FDRs. A stringent significance threshold of FDR < 0.05, coupled with $|\log2(\text{fold change})| \geq 1$, was

judiciously applied to ascertain the significance of DEGs. Finally, KOBAS (version 3.0) software was proficiently employed to accumulate and statistically evaluate the DEGs within the KEGG pathway.

Statistical Analysis

All figures were generated using GraphPad Prism (version 10) software. Data are expressed as the mean ± SD. For data following a normal distribution, parametric tests such as the two-tailed unpaired Student's t-test and one-way ANOVA followed by Tukey's post-hoc test were used. For comparisons involving two independent variables, two-way ANOVA was applied with Bonferroni correction for multiple comparisons. For non-normally distributed data, non-parametric tests such as the Mann-Whitney U test were utilized. Normality was assessed using the Shapiro-Wilk test. The suitability of parametric tests was verified by checking the assumptions of normality and homogeneity of variances. When these assumptions were not met, appropriate non-parametric alternatives were used. Specific statistical tests used for each figure and table are detailed in the respective legends and captions. For example, the Mann-Whitney U test was applied in Table S2 due to the non-normal distribution of the data. A significance level of $p < 0.05$ was considered statistically significant. All experimental conditions were performed in triplicate unless otherwise specified.

RESULTS

Downregulated Expression of ACVR2A in PE Tissues Reveals a Significant Correlation

Several studies have established significant correlations between ACVR2A gene polymorphisms and the susceptibility to pre-eclampsia (PE) in different populations. Table 1 summarizes the key findings from these studies, highlighting the associations between various single nucleotide polymorphisms (SNPs) in the ACVR2A gene and the incidence of PE. These correlations suggest that genetic variations in ACVR2A may play a crucial role in the pathogenesis of PE.

These findings underscore the significance of ACVR2A gene variants in the initiation of PE, particularly in early-onset cases. In this study, placental samples were obtained from 20 patients, and the detailed clinical attributes are presented in Table S1. No significant differences in age and pre-pregnancy BMI were observed between the PE group and the normal control (NC) group ($P > 0.05$). However, the average birth weight of infants delivered by mothers in the PE group was markedly lower than that in the control group ($P < 0.05$).

Analysis of transcriptome data from a public database (accession number: GSE14691) focusing on PE placentas indicated a downward trajectory in ACVR2A expression within the PE group (Figures 1A and 1B). Western blot analysis confirmed notable differences in ACVR2A expression in clinical placental samples obtained from individuals with PE and those with uncomplicated pregnancies (NC, $P < 0.001$, Figure 1C and Figure S1A). RT-PCR findings revealed a significant reduction in ACVR2A mRNA expression within the PE group ($P < 0.001$, Figure 1D). Immunohistochemical (IHC) investigations were carried out on postnatal placental tissue embedded in paraffin to elucidate the spatial distribution of ACVR2A. The signal intensity of ACVR2A in

the NC group was significantly higher than that in the PE group ($P < 0.001$, Figure 1E and Figure S1B). Experimental evidence has indicated predominant expression of HLA-G in trophoblast cells of extravillous trophoblasts, a critical site at the maternal–fetal interface, where trophoblast cells closely interact with the maternal uterine wall [19]. Consequently, immunofluorescence focused on the placental maternal surface, with concurrent staining for ACVR2A and HLA-G. The results of immunofluorescence revealed a diminished signal of ACVR2A in the PE group compared with the NC group, providing additional confirmation of the reduced expression of ACVR2A in PE (Figure 1F and Figure S2).

Precision Genome Surgery: ACVR2A Knockout via CRISPR/Cas9

Preliminary experiments confirmed the expression of ACVR2A in trophoblast cells. The expression of ACVR2A in trophoblast cells was verified using NCBI and The Human Protein Atlas, which further substantiated the experimental findings. The mRNA levels were analyzed using RT-PCR in various cell types, including HTR8/SVneo, JAR, HCoEpiC (human normal colon epithelial cells), 293 human embryonic kidney cells, MEG-01 (human megakaroblastic leukemia cells), Huh-7 (human liver cancer cells), NCI-H358 (human non-small cell lung cancer cells), HaCaT (human immortal epidermal cells), induced pluripotent stem (iPS) cells, A427 (human lung cancer cells), and A549 (human non-small cell lung cancer cells), to understand the expression of ACVR2A in different cell lines. In Figure 2A, the mRNA levels of 293 and iPS cells were lower than those of the other cell lines, whereas the mRNA expression levels of HTR8/SVneo and JAR cells resembled those of other cancer cells.

Notably, the mRNA expression of JAR cells was significantly higher than that of the other cancer cell lines.

Consequently, a potential association between the ACVR2A gene and cell invasion and migration behavior was hypothesized. A comprehensive analysis of ACVR2A expression was conducted in the placentas of women diagnosed with pregnancy-related disorders to delve deeper into the potential connection between abnormal ACVR2A expression and trophoblastic function in pregnancy complications. This approach involved examining the mRNA levels in different cell lines. The results presented in Figure 2A highlighted varying expression patterns across cell types. These findings prompt further exploration into the role of ACVR2A in trophoblastic function and its potential implications for pregnancy-related disorders.

This study focused on the HTR8/SVneo and JAR cell lines, both derived from human extravillous trophoblasts (EVT) cell lines during early pregnancy. Originating from chorionic villi in early pregnancy, the HTR-8/SVneo cell line serves as a prevalent in-vitro model for cultured human cells. Researchers frequently opt for the HTR8/SVneo cell line as an alternative model to investigate placental function and study pregnancy-related diseases.

JAR cell lines derived from placental tissue exhibited heightened sensitivity to morphological and biological changes induced by trophoblastic-specific factors [20]. Given their choriocarcinoma properties, JAR cells offer a valuable model for simulating and studying trophoblast invasion during pregnancy [21]. Thus, JAR and HTR8/SVneo cell lines constituted the cell models employed in the present study.

We employed CRISPR/Cas9 technology to delete the ACVR2A gene in HTR8/SVneo and JAR cell lines. The successful knockout was confirmed through Sanger sequencing, DNA agarose gel electrophoresis, and RT-PCR. This allowed us to investigate the effect of ACVR2A deletion on trophoblast cell behavior[22]. By employing the CRISPR/Cas9 conditional knockout system, two sgRNAs were designed to induce the knockout of the ACVR2A gene in two cell lines through electroporation (Figure 2B). The genotypic fragment resulting from the double sgRNA knockout was 775 bp, and the genotypic fragment of the wild type (WT) measured 1750 bp (Figure S3). Following multiple rounds of monoclonal screening culture, genotype identification, RT-qPCR and Western blotting (WB) analysis for screening, specific double-knockout monoclonal cell lines were distinctly chosen (Figure 2C, $P < 0.001$, Figure 2D-2E). Subsequent Sanger sequencing confirmed this outcome, revealing the successful knockout of the gene segment between the two sgRNAs (Figure 2F, Figure S4, and Figure S5). These experiments helped further investigate the complex process of ACVR2A's involvement in trophoblast function and reveal its potential regulatory role in trophoblast proliferation and invasion. The use of advanced gene manipulation techniques, such as CRISPR/Cas9, ensured the accuracy and validity of the experimental approach, ensuring the successful deletion of ACVR2A in the target cell line. This provides a foundation for further study of the downstream effects and molecular mechanisms of ACVR2A on trophoblastic function.

ACVR2A Knockout Diminishes In-vitro Cell Migration and Invasion

Cells at the periphery of the scratch could progressively migrate into the void,

facilitating the healing of the scratch. The knockout of ACVR2A markedly impeded the migration of HTR8/SVneo and JAR cells in comparison to NCs ($P < 0.001$, Figure 3A). As illustrated in Figure 3B, the ACVR2A gene knockout markedly suppressed the proliferation rate of HTR8/SVneo cells and JAR cells in comparison to NC ($P < 0.001$, Figure 3B). Transwell invasion assays further demonstrated reduced invasive capabilities ($P < 0.001$, Figure 3C). Colony formation assays revealed a significant decrease in clonogenicity in ACVR2A knockout cells ($P < 0.001$, Figure 3D). The experiments established that ACVR2A plays a crucial role in regulating fundamental cell functions, and its knockout markedly hinders cell migration, proliferation, invasion, and clonal formation. The results hold important implications for comprehending the role of ACVR2A in cellular biology and the development of diseases.

RNA-seq Unveils ACVR2A-mediated Regulation of Trophoblast Cell Migration and Invasion via Wnt Pathway

Transcriptome sequencing, also known as RNA-seq, is the latest sequencing technology for comprehensive and rapid transcriptome analysis, providing gene sequence and transcriptomic data for specific cells or tissues of a given species. ACVR2A has been shown to regulate the expression of numerous genes in its proximity. Comprehensive RNA sequencing was performed on both ACVR2A knockout (ACVR2A-KO) and WT cells to uncover the intricate mechanisms through which ACVR2A regulates HTR8/Svneo and JAR cell function. In the JAR knockout group, the deletion of ACVR2A led to the upregulation of 144 genes and the downregulation of 240 genes. By contrast, in the HTR8/Svneo cells, 99 genes were upregulated, and 73

genes were downregulated (Figures 4A and 5A). Gene Set Enrichment Analysis (GSEA) is a computational approach that facilitates the evaluation of the enrichment of predefined gene sets within a sequenced gene list. GSEA serves as a powerful tool that aids researchers in gaining profound insights into genomic data and elucidating crucial genes and pathways involved in biological processes.

GSEA was employed to elucidate the effect of ACVR2A gene knockout on critical genes and biological pathways in cellular systems, and the canonical pathways from the Cancer Genome Project (CGP) database were investigated. The results suggested modifications in several biological pathways. Information from the KEGG website was integrated with the analysis data of this study, uncovering substantial variations in the Wnt signaling pathway. In JAR cells, the NES value was −1.67, with a p-value of 1.03E-04, whereas in HTR8/Svneo cells, the NES value was −1.45, with a p-value of 0.6E-02 (Figures 4B and 5B). Dotplot and centplot visualizations were created, highlighting the connections among at least 10 pathways associated with cell migration and invasion (Figures 4C and 5C). These plots provide insights into the critical genes and biological pathways that ACVR2A may regulate in cellular processes. Detailed gene analysis of specific, related biological pathways is presented in Figures 4D and 5D. Additionally, Figures 4E and 5E visually represent the differentially expressed genes within the Wnt signaling pathway.

ACVR2A Regulates the Migration and Invasion of Trophoblast Cells through TCF7/c-JUN Pathway

Previous experiments have confirmed the pivotal role of ACVR2A in regulating

the fundamental functions of trophoblast cells. Knocking out ACVR2A significantly hindered the migration, proliferation, invasion, and clonal formation of trophoblast cells. The results of RNA-seq analysis showed that ACVR2A knockout resulted in aberrations in multiple signaling pathways, including cell migration, TGF-β, and Wnt. By integrating information from the KEGG website with the analytical data in this study, ACVR2A was identified to potentially regulate the fundamental biological functions of trophoblastic cells through the TCF7/c-JUN signaling pathway. Relevant genes enriched in the TCF7/c-JUN pathway, such as Wnt3, Wnt4, c-JUN, CCND1, TCF7, and TCF7L1, were selected for detailed investigation to further validate the effect of ACVR2A on specific gene expression. The RT-PCR results demonstrated that the mRNA expression levels at tissue and cell levels significantly decreased following ACVR2A knockout compared with the NC group ($p < 0.001$, Figures 6A–C). Additionally, IHC analysis was employed to assess the protein expression levels of TCF7, TCF7L1, and c-JUN in clinical placental samples from PE patients and normal controls. As depicted in Figures 6D–I, the expression levels of these proteins were significantly reduced in the placental tissues from PE patients compared to normal controls. These findings support the hypothesis that reduced ACVR2A expression is associated with altered TCF7/c-JUN pathway activity in PE placental tissues. These findings further illuminate the intricate mechanisms by which ACVR2A regulates the biological functions of trophoblast cells. In conclusion, the diminished expression of ACVR2A significantly influences the proliferation, invasion, and migration of trophoblastic cells in women with PE. The modulation of ACVR2A on HTR-8/SVneo

cell function may be actualized through the TCF7/c-JUN signaling pathway.

DISCUSSION

Pre-eclampsia (PE) is a severe pregnancy complication that significantly risks mothers and fetuses, driven by complex genetic and environmental interactions, and is closely linked to placental abnormalities such as defects in implantation, trophoblast dysfunction, and abnormal vascular development [4, 23]. Advanced maternal age is a notable risk factor, particularly with the trend of delayed childbearing [24-26]. Understanding PE mechanisms and developing suitable models are crucial but challenging due to the unique nature of human placental dysfunction [27]. Trophoblast cells are vital during pregnancy, supporting embryo attachment, decidualization, vascular remodeling, hormone production, and nutrient transport. Their dysfunction is closely linked to PE, making them a key focus in PE research [28]. Most studies, including ours, use trophoblast cells in in-vitro and in-vivo models such as cell lines, placental explants, and animal models to investigate PE mechanisms and pathogenesis.

In recent years, GWASs have achieved significant progress in elucidating the genetic basis of PE. Several risk loci associated with PE, including ACVR2A, MTHFR, and FGF, have been identified [29-31]. In-depth exploration of these genes enhances understanding of individual variations in PE, aiding early prediction, intervention, and treatment. A comprehensive analysis of multiple PE SNP datasets has emphasized the importance of ACVR2A gene variants in the onset of PE, especially in early-onset cases [8-15]. ACVR2A regulates reproductive functions such as decidualization, trophoblastic invasion, and placenta formation, with studies showing abnormal

expression in the decidua of PE patients [32-36]. Studies have found that ACVR2A is abnormally expressed in the decidua of PE patients, further supporting its crucial role [34]. The predominant expression of this receptor in endometrial, placental, and vascular endothelial cells underscores its central role in pregnancy-related mechanisms [18]. Therefore, the present study focused on understanding whether ACVR2A influences the biological behavior of trophoblastic cells during early placental development and how this influence contributes to the development of PE.

To validate the expression of ACVR2A in PE, we initially examined public databases containing transcriptomic data. Transcriptome sequencing analysis revealed low ACVR2A expression in placental samples from PE patients, consistent with GWAS results across diverse populations. We collected placental samples from PE patients and normotensive pregnant women, meticulously washing them to minimize blood cell contamination. Using Western blot, RT-PCR, and immunohistochemistry, we confirmed the low ACVR2A expression in PE placentas. While this association is clear, the precise role of ACVR2A in PE pathogenesis remains to be fully elucidated.

Studies suggested that despite being distinct cell types, tumor and trophoblast cells exhibit similarities in specific biological behaviors, encompassing cell proliferation and growth, cell migration and invasion, abnormal cell signaling pathways, angiogenesis, and immune system evasion [18, 37-39]. Dong et al. discovered that circular RNA ACVR2A is implicated in the invasion and migration of bladder cancer cells [40]. Additional studies indicated that the activin A/ACVR2A axis promotes metastasis in colon cancer by selectively activating SMAD2 [41, 42]. ACVR2A and ALK3 regulate

endometrial receptivity and embryo implantation in mice, with knockout mice showing significant reproductive defects [36]. Ferreira et al. identified a significant association between ACVR2A and early-onset PE [8]. These findings underscore the critical role of ACVR2A in cell growth and development, prompting exploration of its contribution to PE through modulation of abnormal trophoblast invasion. The assessment of ACVR2A mRNA expression levels across multiple cell lines demonstrated that in HTR-8/SVneo and JAR cells, the expression levels of ACVR2A mRNA were comparable to those of tumor cells such as A549. This discovery suggested a potential pivotal role of ACVR2A in the biological functions of trophoblast cells, especially in the nurturing layer. Consequently, further investigation was conducted using these trophoblast cell lines.

CRISPR/Cas9, developed by researchers like George Church and Jennifer Doudna, uses guide RNAs to target specific genomic regions, allowing for precise gene removal, insertion, silencing, or activation, with advantages like complete gene deletion despite potential off-target effects [43-45]. CRISPR/Cas9 technology was used to delete the ACVR2A gene in two trophoblast cell lines to further explore the correlation between PE and ACVR2A. The successful deletion of ACVR2A was confirmed through Sanger sequencing, genotype identification, and RT-PCR. This precise and targeted gene editing allowed validation of the effect of the ACVR2A gene on various trophoblast cell lines. The deletion resulted in suppressed cell growth, impeded migration, and reduced invasion capabilities, highlighting ACVR2A's crucial role in these processes. These findings suggest that ACVR2A plays a significant role in trophoblast cell

functions, which are critical for proper placental development. The observed suppression of cell growth, migration, and invasion upon ACVR2A deletion indicates that this gene is integral to the invasive behavior of trophoblast cells, a process essential for normal placentation and successful pregnancy outcomes.

The regulatory role of ACVR2A may be mediated through the TCF7/c-JUN pathway, as our transcriptome analysis revealed significant downregulation of genes in this pathway following ACVR2A knockout. This connection provides a potential mechanistic link between ACVR2A expression and trophoblast cell behavior. RT-PCR was conducted to confirm the mRNA expression levels of Wnt3, Wnt4, c-JUN, CCND1, TCF7, and TCF7L1 to validate the results of the RNA-seq data analysis. The results demonstrated a significant downregulation of these six genes in HTR-8/SVneo-ACVR2A-KO and JAR-ACVR2A-KO. The downregulation of Wnt pathway-related genes further supported the concept of ACVR2A influencing trophoblast cell function through various and complex mechanisms. In placental samples from patients with PE and normotensive pregnant women, lower expression levels of these six genes were observed in the PE group, with immunohistochemistry results highlighting a particularly significant decrease in TCF7L1. Consistent with previous studies, this research supported the downregulation of Wnt3, Wnt4, c-JUN, CCND1, TCF7, and TCF7L1 in PE [47]. These findings suggest that ACVR2A plays a significant role in trophoblast cell functions, critical for proper placental development.

In conclusion, our study provides new insights into the role of ACVR2A in trophoblast cells and its broader implications in pregnancy-related disorders. Future

research should focus on exploring the specific molecular interactions of ACVR2A within the TCF7/c-JUN pathway and other related signaling pathways to develop targeted therapies for PE. These findings advance our understanding of PE pathogenesis and suggest potential avenues for therapeutic intervention.

Competing interests

The authors declare that they have no competing interests.

Ethics approval and consent to participate

All participants in this study provided a written informed consent for donating blood. The Ethics Committee of The Third Affiliated Hospital of Guangzhou Medical University (Guangzhou, China) approved the experiments using human cells. The animal experiments were approved by The Third Affiliated Hospital of Guangzhou Medical University. All methods were performed in accordance with the approved guidelines.

Authors' contributions

Shujing Yang and Huanyao Liu designed the experiments, conducted most of the experiments, and analyzed the results. Yi Yang participated in the study design and wrote the article. Bingjun Chen, Wanlu An and Xuwen Song participated in the process of experiment. Shujing Yang and Jieshi Hu collected the sample and performed the statistical analysis. Fang He provided parts of the experimental materials. Fang He and Yi Yang performed the quality control of this study.

Funding

This study was supported by the Guangdong Basic and Applied Basic Research Fund

(Guangdong-Shenzhen Joint Fund) (2021B1515120070, 2023A1515010872), the National Key R&D Program of China (2021YFC2701500, 2019YFA0110804), Guangzhou fundamental research project jointly funded by School (Institution)(high-level university) (202102010131)

REFERENCES

1. Chen, X., et al., *Gut dysbiosis induces the development of pre-eclampsia through bacterial translocation.* Gut, 2020. **69**(3): p. 513-522.
2. *Pre-eclampsia.* Nat Rev Dis Primers, 2023. **9**(1): p. 9.
3. Gebara, N., et al., *Angiogenic Properties of Placenta-Derived Extracellular Vesicles in Normal Pregnancy and in Preeclampsia.* Int J Mol Sci, 2021. **22**(10).
4. Chappell, L.C., et al., *Pre-eclampsia.* Lancet, 2021. **398**(10297): p. 341-354.
5. Hua, H., *From GWAS to single-cell MPRA.* Nat Methods, 2023. **20**(3): p. 349.
6. Li, P., et al., *Association between gut microbiota and preeclampsia-eclampsia: a two-sample Mendelian randomization study.* BMC Med, 2022. **20**(1): p. 443.
7. Yong, H.E.J., et al., *Genetic Approaches in Preeclampsia.* Methods Mol Biol, 2018. **1710**: p. 53-72.
8. Ferreira, L.C., et al., *Association between ACVR2A and early-onset preeclampsia: replication study in a Northeastern Brazilian population.* Placenta, 2015. **36**(2): p. 186-90.
9. Yanan, F., et al., *Association between ACVR2A gene polymorphisms and risk of hypertensive disorders of pregnancy in the northern Chinese population.* Placenta, 2020. **90**: p. 1-8.
10. Roten, L.T., et al., *Association between the candidate susceptibility gene ACVR2A on chromosome 2q22 and pre-eclampsia in a large Norwegian population-based study (the HUNT study).* Eur J Hum Genet, 2009. **17**(2): p. 250-7.
11. Fitzpatrick, E., et al., *Genetic association of the activin A receptor gene (ACVR2A) and pre-eclampsia.* Mol Hum Reprod, 2009. **15**(3): p. 195-204.
12. Amosco, M.D., et al., *Non-additive effects of ACVR2A in preeclampsia in a Philippine population.* BMC Pregnancy Childbirth, 2019. **19**(1): p. 11.
13. Moses, E.K., et al., *Objective prioritization of positional candidate genes at a quantitative trait locus for pre-eclampsia on 2q22.* Mol Hum Reprod, 2006. **12**(8): p. 505-12.
14. Zeybek, B., et al., *Polymorphisms in the activin A receptor type 2A gene affect the onset time and severity of preeclampsia in the Turkish population.* J Perinat Med, 2013. **41**(4): p. 389-99.
15. Glotov, A.S., et al., *Targeted sequencing analysis of ACVR2A gene identifies novel risk variants associated with preeclampsia.* J Matern Fetal Neonatal Med, 2019. **32**(17): p. 2790-2796.
16. Dean, M., D.A. Davis, and J.E. Burdette, *Activin A stimulates migration of the fallopian tube*

epithelium, an origin of high-grade serous ovarian cancer, through non-canonical signaling. Cancer Lett, 2017. **391**: p. 114-124.

17. Yong, H.E., et al., *Effects of normal and high circulating concentrations of activin A on vascular endothelial cell functions and vasoactive factor production.* Pregnancy Hypertens, 2015. **5**(4): p. 346-53.
18. Lokki, A.I., et al., *Association of the rs1424954 polymorphism of the ACVR2A gene with the risk of pre-eclampsia is not replicated in a Finnish study population.* BMC Res Notes, 2011. **4**: p. 545.
19. Ferreira, L.M.R., et al., *HLA-G: At the Interface of Maternal-Fetal Tolerance.* Trends Immunol, 2017. **38**(4): p. 272-286.
20. Zeng, H.J., et al., *Studies on the anti-aging activity of a glycoprotein isolated from Fupenzi (Rubus chingii Hu.) and its regulation on klotho gene expression in mice kidney.* Int J Biol Macromol, 2018. **119**: p. 470-476.
21. Alvarez-Cienfuegos, A., et al., *FGF23-Klotho axis in patients with rheumatoid arthritis.* Clin Exp Rheumatol, 2020. **38**(1): p. 50-57.
22. Jinek, M., et al., *A programmable dual-RNA-guided DNA endonuclease in adaptive bacterial immunity.* Science, 2012. **337**(6096): p. 816-21.
23. Steegers, E.A., et al., *Pre-eclampsia.* Lancet, 2010. **376**(9741): p. 631-44.
24. Miller, E.C., et al., *Pregnancy, preeclampsia and maternal aging: From epidemiology to functional genomics.* Ageing Res Rev, 2022. **73**: p. 101535.
25. Bartsch, E., et al., *Clinical risk factors for pre-eclampsia determined in early pregnancy: systematic review and meta-analysis of large cohort studies.* BMJ, 2016. **353**: p. i1753.
26. Smithson, S.D., N.H. Greene, and T.F. Esakoff, *Pregnancy outcomes in very advanced maternal age women.* Am J Obstet Gynecol MFM, 2022. **4**(1): p. 100491.
27. Carter, A.M., *Comparative studies of placentation and immunology in non-human primates suggest a scenario for the evolution of deep trophoblast invasion and an explanation for human pregnancy disorders.* Reproduction, 2011. **141**(4): p. 391-6.
28. Knofler, M., et al., *Human placenta and trophoblast development: key molecular mechanisms and model systems.* Cell Mol Life Sci, 2019. **76**(18): p. 3479-3496.
29. Tyrmi, J.S., et al., *Genetic Risk Factors Associated With Preeclampsia and Hypertensive Disorders of Pregnancy.* JAMA Cardiol, 2023. **8**(7): p. 674-683.
30. Salonen Ros, H., et al., *Genetic effects on the liability of developing pre-eclampsia and gestational hypertension.* Am J Med Genet, 2000. **91**(4): p. 256-60.
31. Cnattingius, S., et al., *Maternal and fetal genetic factors account for most of familial aggregation of preeclampsia: a population-based Swedish cohort study.* Am J Med Genet A, 2004. **130A**(4): p. 365-71.
32. Manohar-Sindhu, S., et al., *Diminished vasculogenesis under inflammatory conditions is mediated by Activin A.* Angiogenesis, 2023. **26**(3): p. 423-436.
33. Funghi, L., et al., *Placental and maternal serum activin A in spontaneous and induced labor in late-term pregnancy.* J Endocrinol Invest, 2018. **41**(2): p. 171-177.
34. Yong, H.E.J., et al., *Decidual ACVR2A regulates extravillous trophoblast functions of adhesion, proliferation, migration and invasion in vitro.* Pregnancy Hypertens, 2018. **12**: p. 189-193.
35. Pinyol, R., et al., *Molecular characterisation of hepatocellular carcinoma in patients with*

non-alcoholic steatohepatitis. J Hepatol, 2021. **75**(4): p. 865-878.

36. Monsivais, D., et al., *Endometrial receptivity and implantation require uterine BMP signaling through an ACVR2A-SMAD1/SMAD5 axis.* Nat Commun, 2021. **12**(1): p. 3386.
37. Kshitiz, et al., *Evolution of placental invasion and cancer metastasis are causally linked.* Nat Ecol Evol, 2019. **3**(12): p. 1743-1753.
38. Perez-Garcia, V., et al., *BAP1/ASXL complex modulation regulates epithelial-mesenchymal transition during trophoblast differentiation and invasion.* Elife, 2021. **10**.
39. Costanzo, V., et al., *Exploring the links between cancer and placenta development.* Open Biology, 2018.
40. Dong, W., et al. , *Circular RNA ACVR2A suppresses bladder cancer cells proliferation and metastasis through miR-626EYA4 axis.* Molecular Cancer, 2019.
41. Zhang, H., et al., *Activin A/ACVR2A axis inhibits epithelial-to-mesenchymal transition in colon cancer by activating SMAD2.* Molecular Carcinogenesis, 2023. **62**(10): p. 1585-1598.
42. Zhuo, C., et al., *Downregulation of Activin A Receptor Type 2A Is Associated with Metastatic Potential and Poor Prognosis of Colon Cancer.* Journal of Cancer, 2018. **9**(19): p. 3626-3633.
43. Lingor, P., *Regulation of Cell Death and Survival by RNA Interference – The Roles of miRNA and siRNA*, in *Apoptosome*. 2010. p. 95-117.
44. Schuster, A., et al., *RNAi/CRISPR Screens: from a Pool to a Valid Hit.* Trends Biotechnol, 2019. **37**(1): p. 38-55.
45. Manghwar, H., et al., *CRISPR/Cas System: Recent Advances and Future Prospects for Genome Editing.* Trends Plant Sci, 2019. **24**(12): p. 1102-1125.

Figure legends

Figure 1. ACVR2A was downregulated in placental tissue associated with pre-eclampsia.

(A) Comparison of the RNA-seq volcano maps of all genes in the placenta of normal control (NC) and patients with pre-eclampsia (PE) evidently showed that the expression of the ACVR2A gene significantly decreased in patients with PE.

(B) Heat maps depicting the aberrant gene pathways in the NC and PE placentas revealed a decreased expression of the ACVR2A gene in patients with PE compared with NC.

(C) Western blot analysis demonstrated reduced levels of ACVR2A in preeclampsia

placental tissue (n = 10) compared with control placentas.

(D) RT-qPCR was employed to assess the ACVR2A mRNA expression in placental tissues of normal control (NC, n = 10) and patients with pre-eclampsia (PE, n = 10).

(E) Immunohistochemical staining was conducted using rabbit IgG anti-human ACVR2A antibody on sections from normal control and pre-eclampsia (PE) placentas. Sections were counterstained with hematoxylin. The ACVR2A levels were markedly lower in patients with PE (n = 10) than in NC.

(F) Immunofluorescence co-localization of rabbit IgG anti-human ACVR2A antibodies and HLA-G antibodies (a marker of extrachorionic trophoblastic cells) was performed in normal control and pre-eclampsia maternal placenta. The expression pattern of the ACVR2A antibody closely resembles that of the HLA-G antibody, primarily expressed in EVT cells.

(*P < 0.05, **P < 0.01, ***P < 0.001, and ****P < 0.0001 compared with normal control group).

Figure 2. The ACVR2A gene in JAR and HTR8/SVneo cells was successfully knocked out using CRISPR/Cas9 gene editing technology.

(A) RT-qPCR was employed to assess the ACVR2A mRNA expression across various cell lines. The expression of ACVR2A in HTR8/SVneo and JAR was comparable to that in multiple cancer cell lines, with JAR exhibiting a higher ACVR2A expression.

(B) DNA sequence of ACVR2A and target sequence site information of sgRNA-1 and sgRNA-2.

(C) The knockout efficiency of the ACVR2A gene in HTR8/SVneo and JAR cell lines

was assessed through polymeric primer PCR, confirmed by agarose gel electrophoresis, and reconfirmed through four rounds of monoclonal cell communities. The specific experimental results are shown in Figure S3.

(D) The ACVR2A mRNA levels were measured in HTR8/SVneo and JAR cell lines, and the normal control group was compared with the two ACVR2A-KO cell lines after three rounds of validation (*P < 0.05, **P < 0.01, ***P < 0.001, and ****P < 0.0001 compared with normal control group).

(E) Western blot analysis showing ACVR2A protein levels in wild-type (WT) and knockout (KO) HTR8/SVneo and JAR cell lines. The ACVR2A protein is significantly absent in KO cell lines compared to WT, confirming successful knockout of the ACVR2A gene.

(F) Sanger sequencing confirmed the expression of ACVR2A in ACVR2A-KO monoclonal cell lines and successfully knocked out the DNA fragment between the ACVR2A gene sgRNA-1 and sgRNA-2. The specific experimental results are shown in Figure S4 and S5.

Figure 3. The invasion, migration, and proliferation in JAR and HTR8/SVneo cells were suppressed following ACVR2A knockout.

(A) Cell scratch assay was conducted in a six-well plate to assess alterations in the migration ability of HTR8/SVneo and JAR cells following ACVR2A gene knockout. Three visual fields were randomly selected under a 100× microscope for continuous observation, calculation, and difference analysis. Scale bar: 100 μm.

(B) CCK-8 method was employed to assess the proliferation of HTR8/SVneo and JAR

cells after ACVR2A gene knockout.

(C) The alterations in the invasion ability of HTR8/SVneo and JAR cells after ACVR2A gene knockout were determined using Transwell invasion assay (100× magnification), with three fields randomly selected under a 300× microscope for counting and statistical analysis. Scale bar: 200μm.

(D) Colony formation was detected by single-cell clone assay. Colony formation assay conducted in a six-well plate to assess changes in the individual cell proliferation capacity of HTR8/SVneo and JAR cells following ACVR2A gene knockout (*P < 0.05, **P < 0.01, ***P < 0.001, and ****P < 0.0001 compared with normal control group).

Figure 4. Transcriptomic analysis revealed that ACVR2A may suppress cell biological behavior through the Wnt/TCF7 pathway in JAR cell lines.

(A) The Volcano plots of RNA-seq for all the genes compared JAR-ACVR2A-KO and WT.

(B) One representative hallmark pathway, the Wnt pathway, in the ACVR2A-KO group.

(C) The enriched biological process pathways of cell invasion and migration based on DEGs (p value cutoff = 0.05).

(D) The category netplot depicted the linkages of downregulated genes and three biological concepts that are related to ACVR2A as a network.

(E) The heatmap showed differentially expressed genes (DEGs) in the Wnt pathway between experimental and normal control groups. Red and blue represent significantly upregulated and downregulated genes, respectively.

Figure 5. Transcriptomic analysis revealed that ACVR2A may suppress cell

biological behavior through the Wnt/TCF7 pathway in HTR8/SVneo cell lines.

(A) Volcano plots of RNA-seq for all the genes compared HTR8/SVneo-ACVR2A-KO and WT.

(B) One representative hallmark pathway, the Wnt pathway, in the ACVR2A-KO group.

(C) The enriched biological process pathways in cell invasion and migration based on DEGs (p value cutoff = 0.05).

(D) The category netplot depicted the linkages of downregulated genes and three biological concepts that are related to ACVR2A as a network.

(E) Heatmap of differentially expressed genes (DEGs) about Wnt pathway between experimental and normal control groups. Red and blue represent significantly upregulated and downregulated genes, respectively.

Figure 6. RT-PCR and immunohistochemistry validated that ACVR2A modulates cellular behavior via the TCF7/c-JUN pathway.

(A) RT-qPCR analysis of DEGs (Wnt3, Wnt4, TCF7, TCF7L1, CCND1, and c-JUN) expression enriched in Wnt/TCF pathway following HTR8/SVneo ACVR2A knockout.

(B) RT-qPCR analysis of DEGs (Wnt3, Wnt4, TCF7, TCF7L1, CCND1, and c-JUN) expression enriched in Wnt/TCF pathway following JAR ACVR2A knockout.

(C) RT-qPCR analysis of DEGs (Wnt3, Wnt4, TCF7, TCF7L1, CCND1, and c-JUN) expression enriched in Wnt/TCF pathway expression in the placenta of normal control pregnant women (NC) and patients with preeclampsia (PE).

(D) Immunohistochemical staining of normal control pregnant women and preeclampsia placentas using rabbit IgG anti-human Wnt3, Wnt4, TCF7L1, TCF7L2,

CCND1, and c-JUN antibody. Sections were counterstained with hematoxylin, and positive cells were quantified using ImageJ software.

Figure 7. The inhibitory effect of ACVR2A on trophoblast cell invasion, migration, and proliferation through the TCF7/c-JUN pathway is illustrated. (Colors: Green: Normal conditions and functional pathways. Red: Abnormalities or disrupted pathways in preeclampsia. Arrows: Solid Dark Brown Arrows: Normal signaling pathways and interactions. Bold Red Arrows: Disrupted or abnormal signaling pathways in preeclampsia.) The typical WNT pathways are intricately connected with ACVR2A and TGFβ. ACVR2A influences TCF7 transcriptional activation via the SMAD1/SMAD5-SMAD4 axis, subsequently affecting genes, such as JUN, CCND1, and others, and ultimately leading to the regulation of trophoblastic cell invasion, migration, and proliferation (draw by FigDraw).

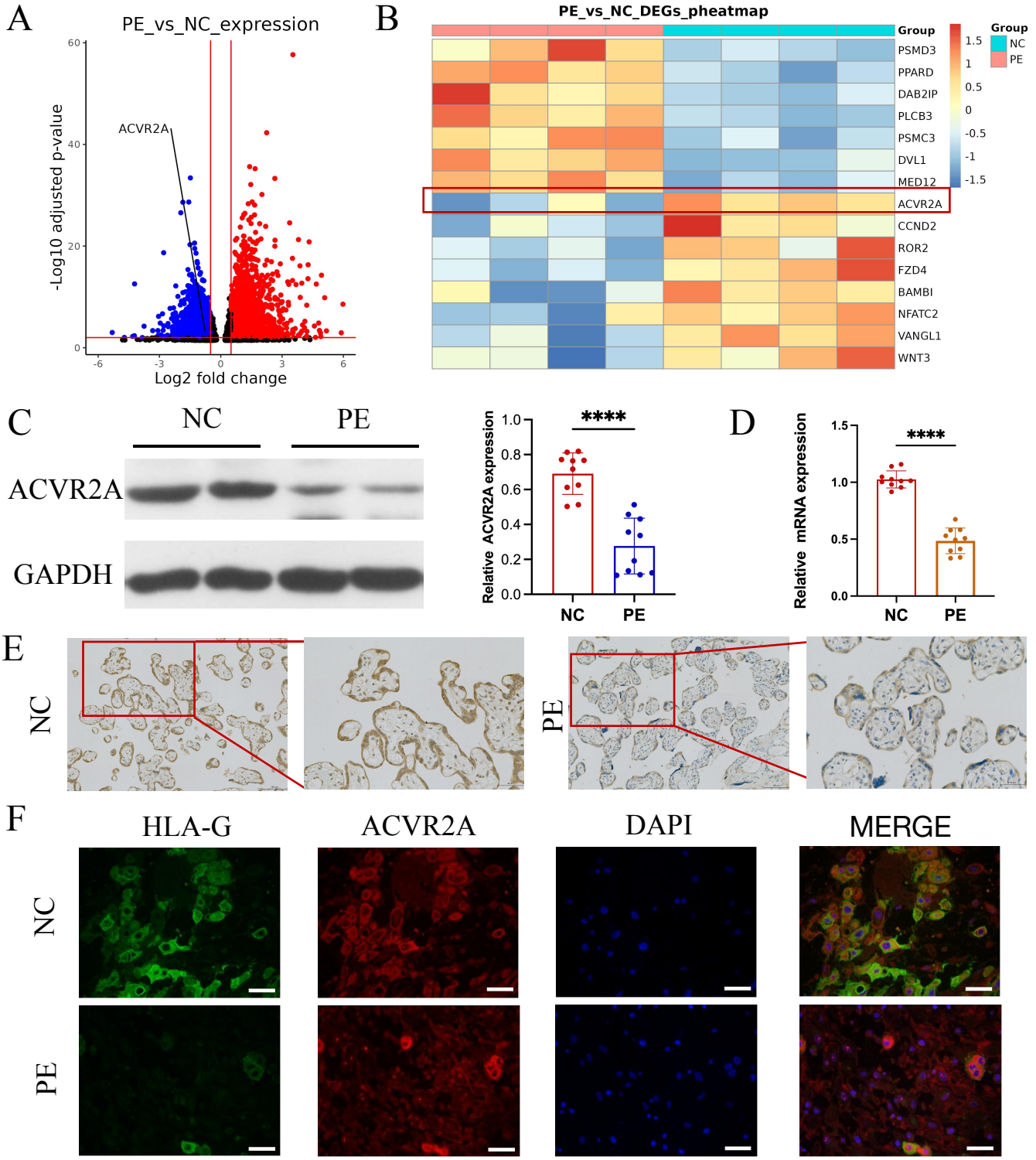

Figure 1. Downregulation of ACVR2A in Placental Tissue Associated with Preeclampsia.
(A) Comparing RNA-seq volcano maps of all genes in the placenta of normal control pregnant women (NC) and preeclampsia patients (PE), it is evident that the expression of the ACVR2A gene is significantly decreased in preeclampsia.
(B) Heat maps depicting these aberrant gene pathways in the NC and PE placentas revealed a decreased expression of the ACVR2A gene in preeclampsia compared to the control group.
(C) Western blot analysis demonstrated reduced levels of ACVR2A in preeclampsia placental tissue (n = 10) compared to control placentas.
(D) qRT-PCR was employed to assess ACVR2A mRNA expression in placental tissues of normal control pregnant women (NC) and preeclampsia patients (PE) (n = 10).
(E) Immunohistochemical staining using rabbit IgG anti-human ACVR2A antibody on sections from normal control pregnant women and preeclampsia placentas. Sections were counterstained with hematoxylin. ACVR2A levels were markedly lower in patients with preeclampsia (n = 10) compared to normal control subjects.
(F) Immunofluorescence co-localization of rabbit IgG anti-human ACVR2A antibodies and HLA-G antibodies (a marker of extrachorionic trophoblastic cells) in normal control and preeclampsia maternal placenta. The expression pattern of the ACVR2A antibody closely resembles that of the HLA-G antibody, primarily expressed in EVT cells.
(*P < 0.05, **P < 0.01, ***P < 0.001, ****P < 0.0001, compared to the control group)

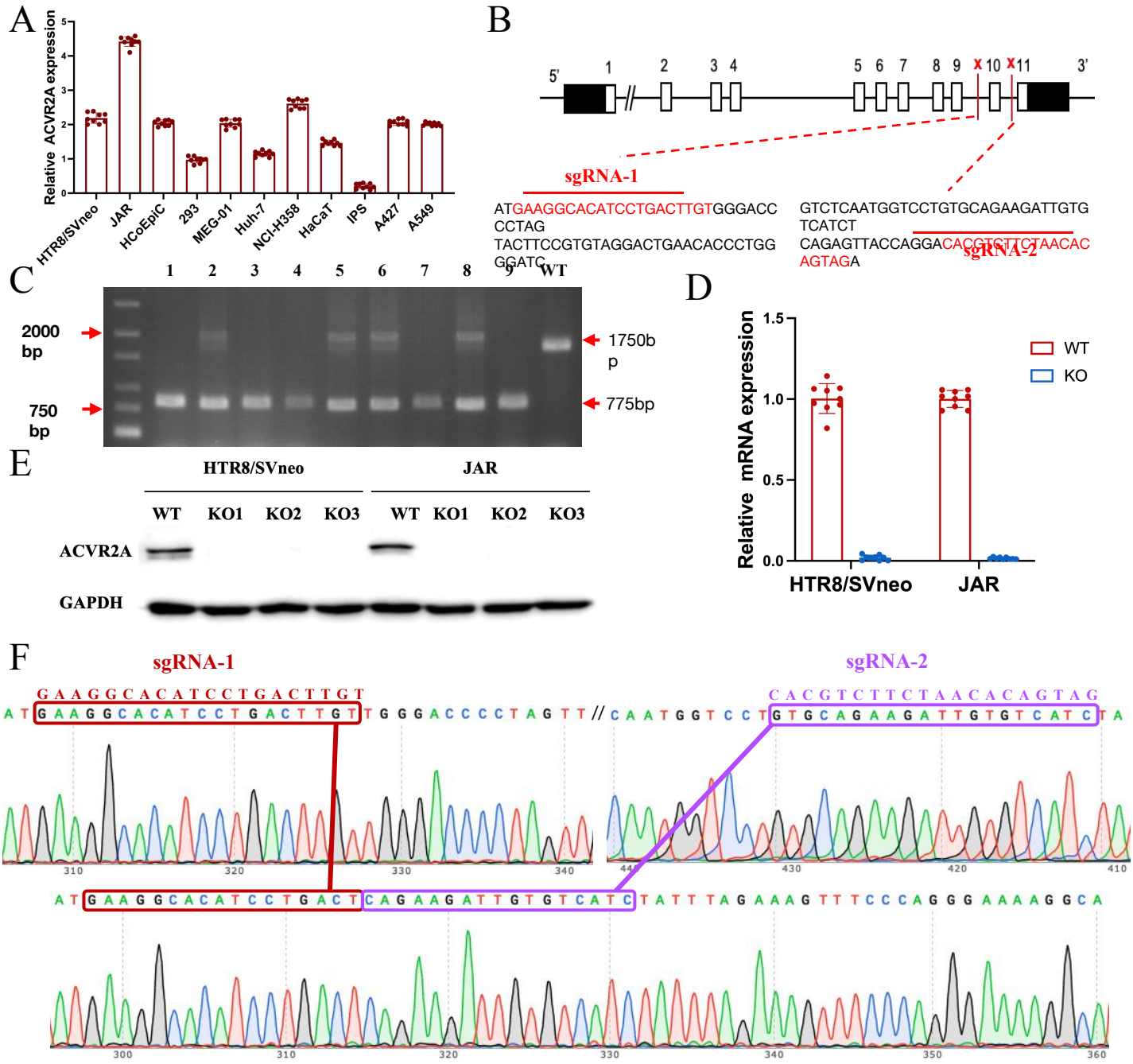

Figure 2. Successful ACVR2A Gene Knockout in JAR and HTR8/SVneo Cells Utilizing CRISPR/Cas9 Gene Editing Technology.

(A) qRT-PCR was employed to assess ACVR2A mRNA expression across various cell lines, including HTR8/SVneo, JAR, HCoEpiC (human normal colon epithelial cells), 293 human embryonic kidney cells, MEG-01 (human megakaryoblastic leukemia cells), Huh-7 (human liver cancer cells), NCI-H358 (human non-small cell lung cancer cells), HaCaT (human immortal epidermal cells), iPS (induced pluripotent stem cells), A427 (human lung cancer cells), and A549 (human non-small cell lung cancer cells). The expression level of ACVR2A in HTR8/SVneo and JAR is comparable to that in multiple cancer cell lines, with JAR exhibiting an even higher expression level.

(B) DNA sequence of ACVR2A and target sequence site information of sgRNA-1 and sgRNA-2.

(C) The knockout efficiency of the ACVR2A gene in HTR8/SVneo and JAR cell lines was assessed through polymeric primer PCR, confirmed by agarose gel electrophoresis, and reconfirmed through four rounds of monoclonal cell communities. Specific experimental results are shown in Figure S3.

(D) ACVR2A mRNA levels were measured in HTR8/SVneo and JAR cell lines, and the control group was compared with the two ACVR2A-KO cell lines after three rounds of validation. (*P < 0.05, **P < 0.01, ***P < 0.001, ****P < 0.0001, compared to the control group)

(E) Western blot analysis showing ACVR2A protein levels in wild-type (WT) and knockout (KO) HTR8/SVneo and JAR cell lines. The ACVR2A protein is significantly absent in KO cell lines compared to WT, confirming successful knockout of the ACVR2A gene.

(F) Sanger sequencing confirmed the expression of ACVR2A in ACVR2A-KO monoclonal cell lines and successfully knocked out the DNA fragment between the ACVR2A gene sgRNA-1 and sgRNA-2. The specific experimental results are shown in Figure S4-S5.

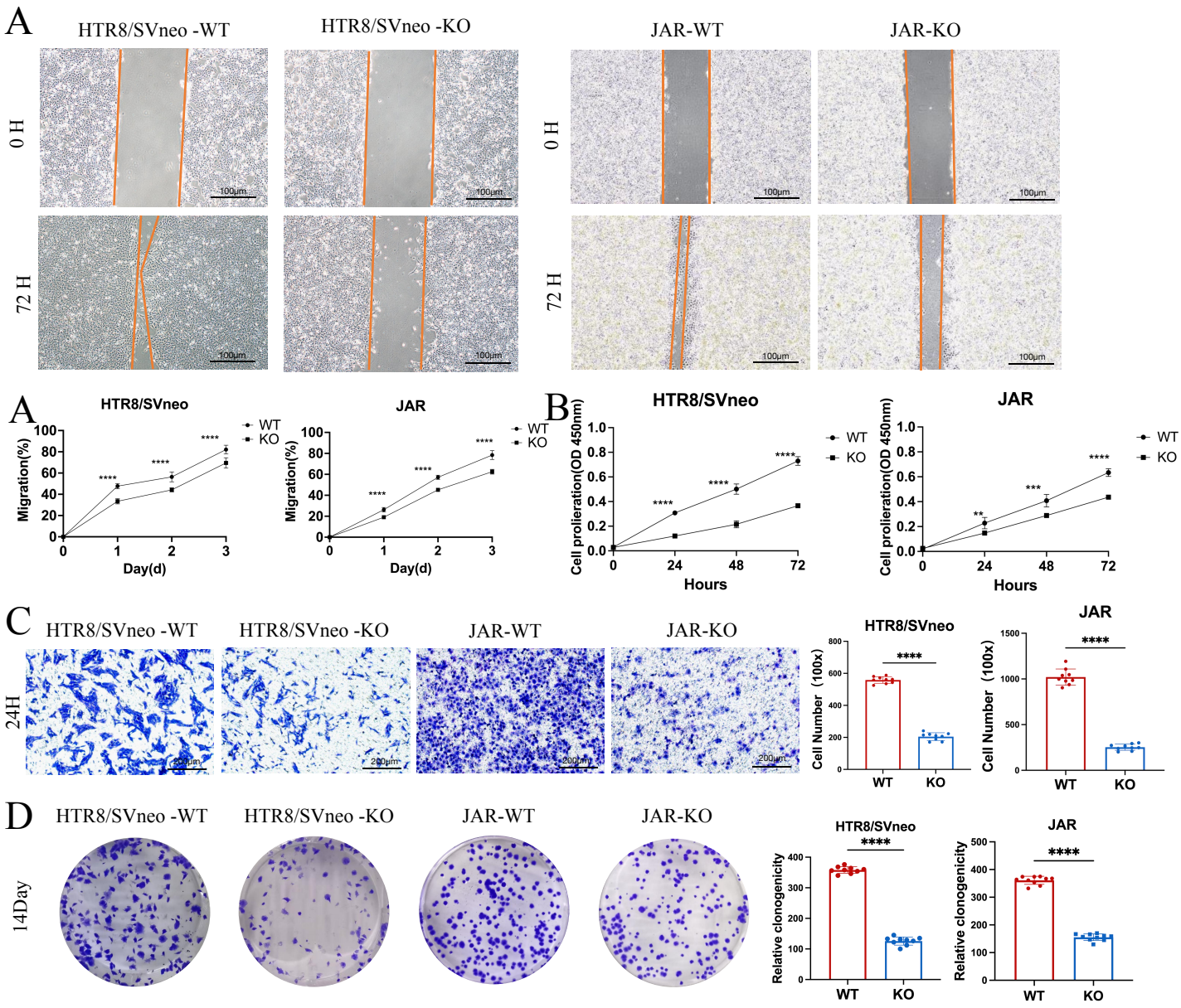

Figure 3. Suppression of Invasion, Migration, and Proliferation in JAR and HTR8/SVneo Cells Following ACVR2A Knockout.

(A) Cell scratch assay was conducted in a 6-well plate to assess alterations in the migration ability of HTR8/SVneo and JAR cells following ACVR2A gene knockout. Three visual fields were randomly selected under a 100x microscope for continuous observation, calculation, and difference analysis; scale bar: 100μm.

(B) The CCK-8 method was employed to assess the proliferation of HTR8/SVneo and JAR cells post ACVR2A gene knockout.

(C) Alterations in the invasion ability of HTR8/SVneo and JAR cells after ACVR2A gene knockout were determined using the Transwell invasion assay (100x magnification), with three fields randomly selected under a 300x microscope for counting and statistical analysis; scale bar: 200μm.

(D) Colony formation was detected by single-cell clone assay. Colony formation were conducted in a 6-well plate to assess changes in the individual cell proliferation capacity of HTR8/SVneo and JAR cells following ACVR2A gene knockout.

(*P < 0.05, **P < 0.01, ***P < 0.001, ****P < 0.0001, compared to the control group)

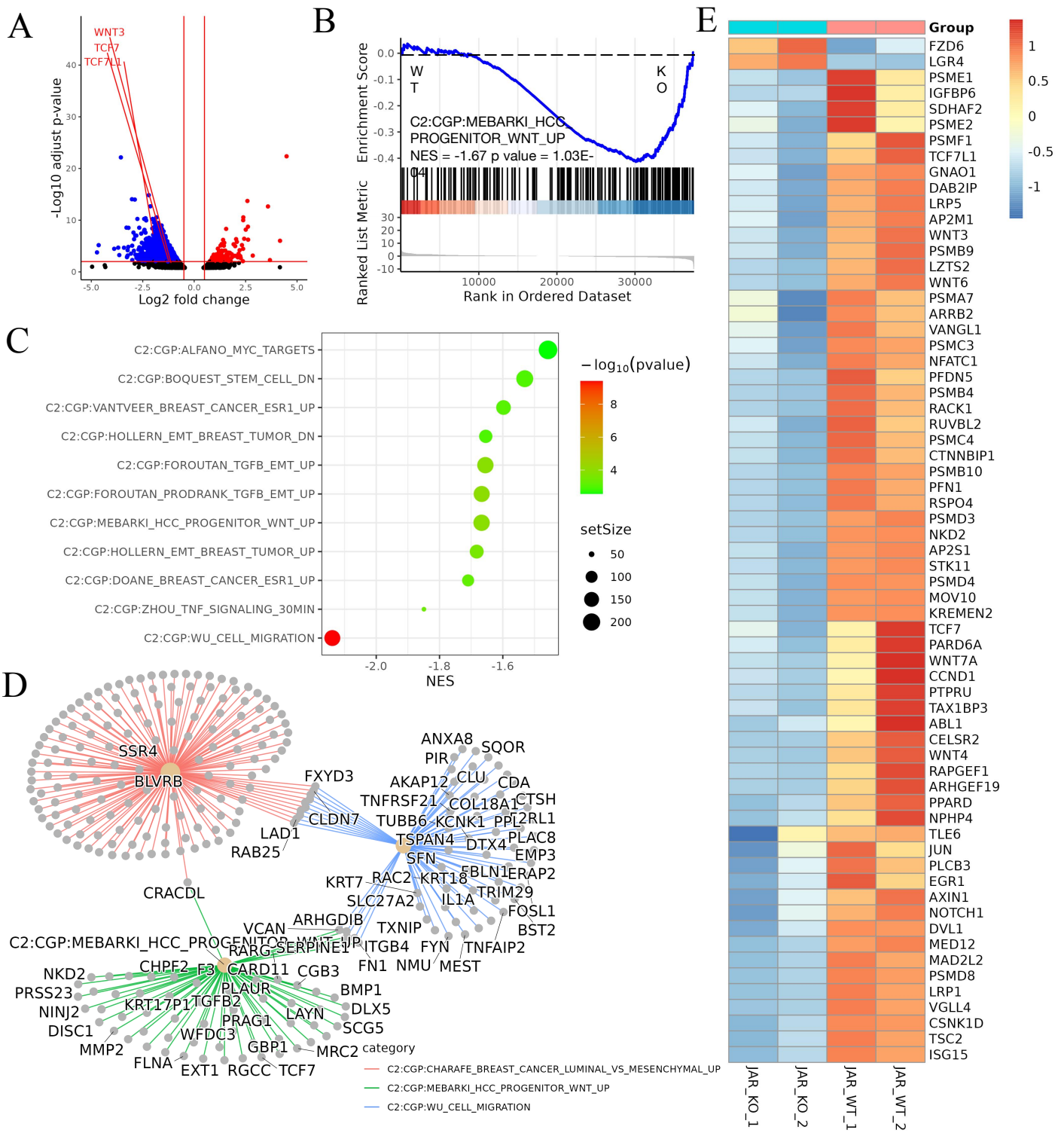

Figure 4. In JAR Cell Lines, Transcriptomic Analysis Reveals that ACVR2A May Suppress Cell Biological Behavior through the WNT/TCF7 Pathway.

(A)A Volcano plots of RNA-seq for all the genes comparing JAR-ACVR2A-KO and WT.

(B)One representative hallmark pathways WNT pathway in the ACVR2A-KO group.

(C) The enriched biological process pathways about invasion and migration based on DEGs (p value Cutoff = 0.05).

(D) The category netplot depicted the linkages of downregulated genes and three biological concepts that are related to ACVR2A as a network.

(E)Heatmap of differential expression genes (DEGs) about WNT pathway between experimental and control group. Red and blue represent the significantly up-regulated and down-regulated genes respectively.

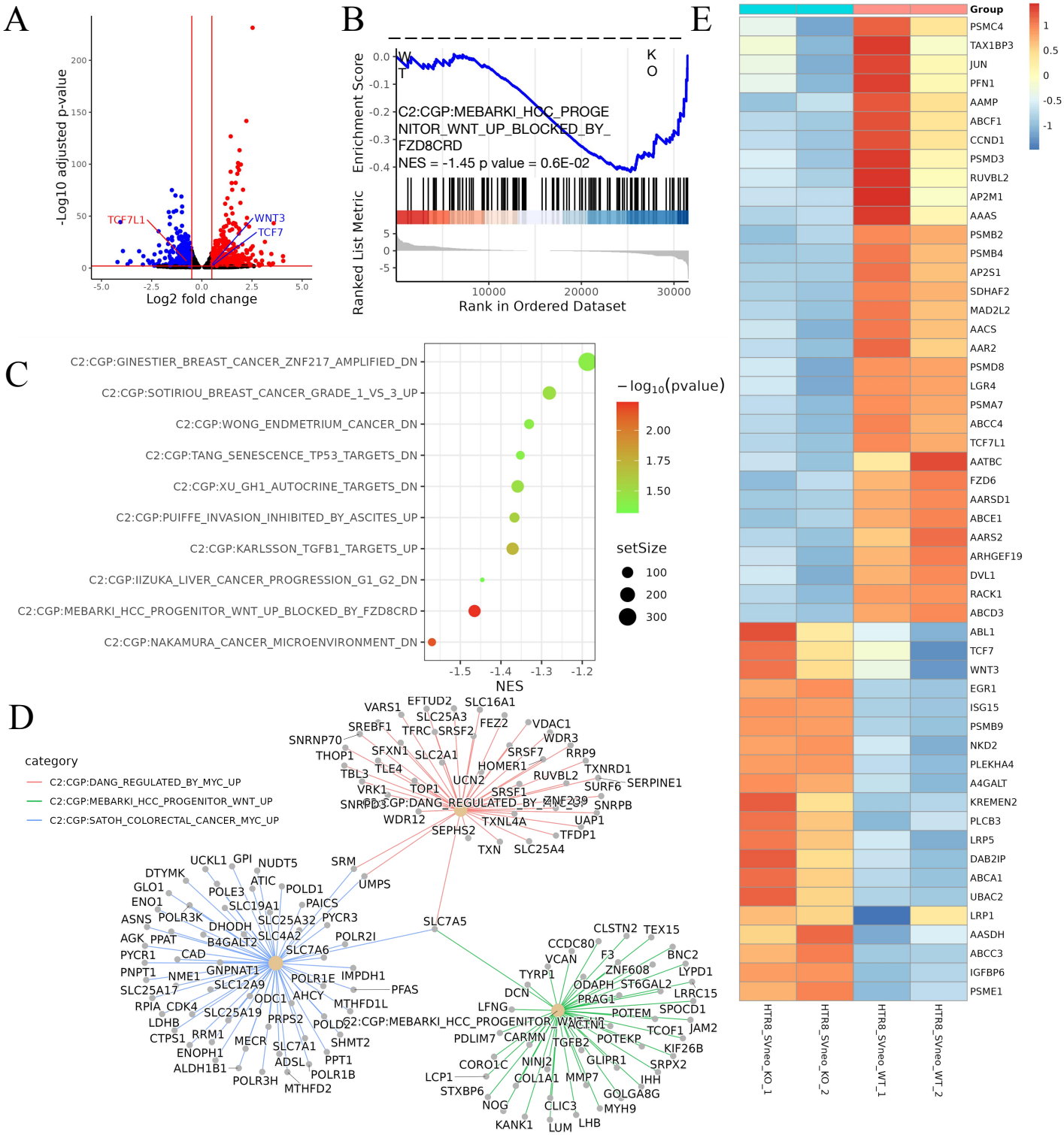

Figure 5. In HTR8/SVneo Cell Line, Transcriptomic Analysis Reveals that ACVR2A May Suppress Cell Biological Behavior through the WNT/TCF7 Pathway.

(A)A Volcano plots of RNA-seq for all the genes comparing HTR-8/SVneo-ACVR2A-KO and WT.

(B)One representative hallmark pathways WNT pathway in the ACVR2A-KO group.

(C) The enriched biological process pathways about invasion and migration based on DEGs (p value Cutoff = 0.05).

(D) The category netplot depicted the linkages of downregulated genes and three biological concepts that are related to ACVR2A as a network.

(E)Heatmap of differential expression genes (DEGs) about WNT pathway between experimental and control group. Red and blue represent the significantly up-regulated and down-regulated genes respectively.

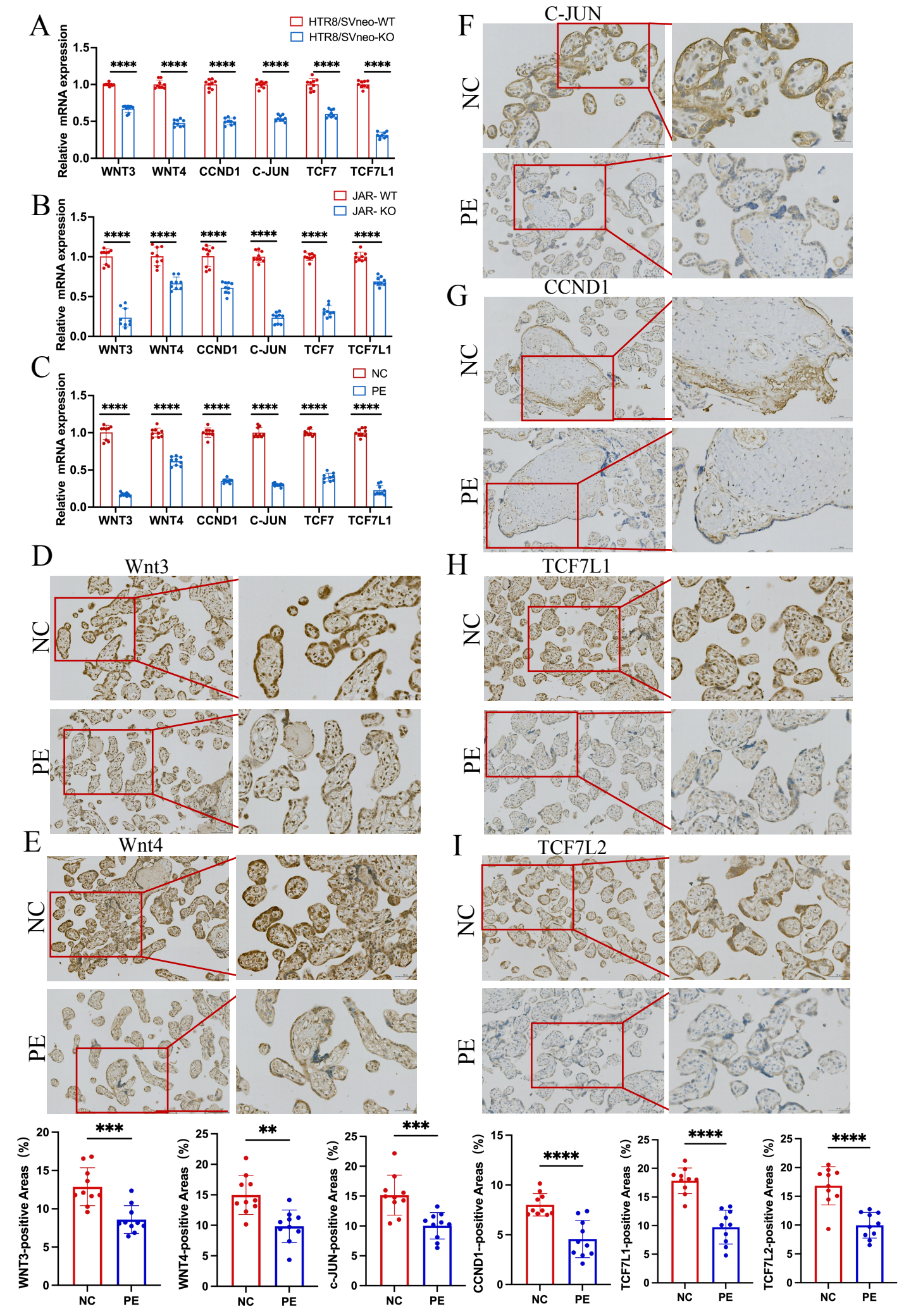
A
HTR8/SVneo-WT
HTR8/SVneo-KO
Relative mRNA expression
WNT3
WNT4
CCND1
C-JUN
TCF7
TCF7L1
B
JAR- WT
JAR- KO
C
NC
PE
D
Wnt3
E
Wnt4
F
C-JUN
G
CCND1
H
TCF7L1
I
TCF7L2
WNT3-positive Areas (%)
WNT4-positive Areas (%)
c-JUN-positive Areas (%)
CCND1--positive Areas (%)
TCF7L1-positive Areas (%)
TCF7L2-positive Areas (%)

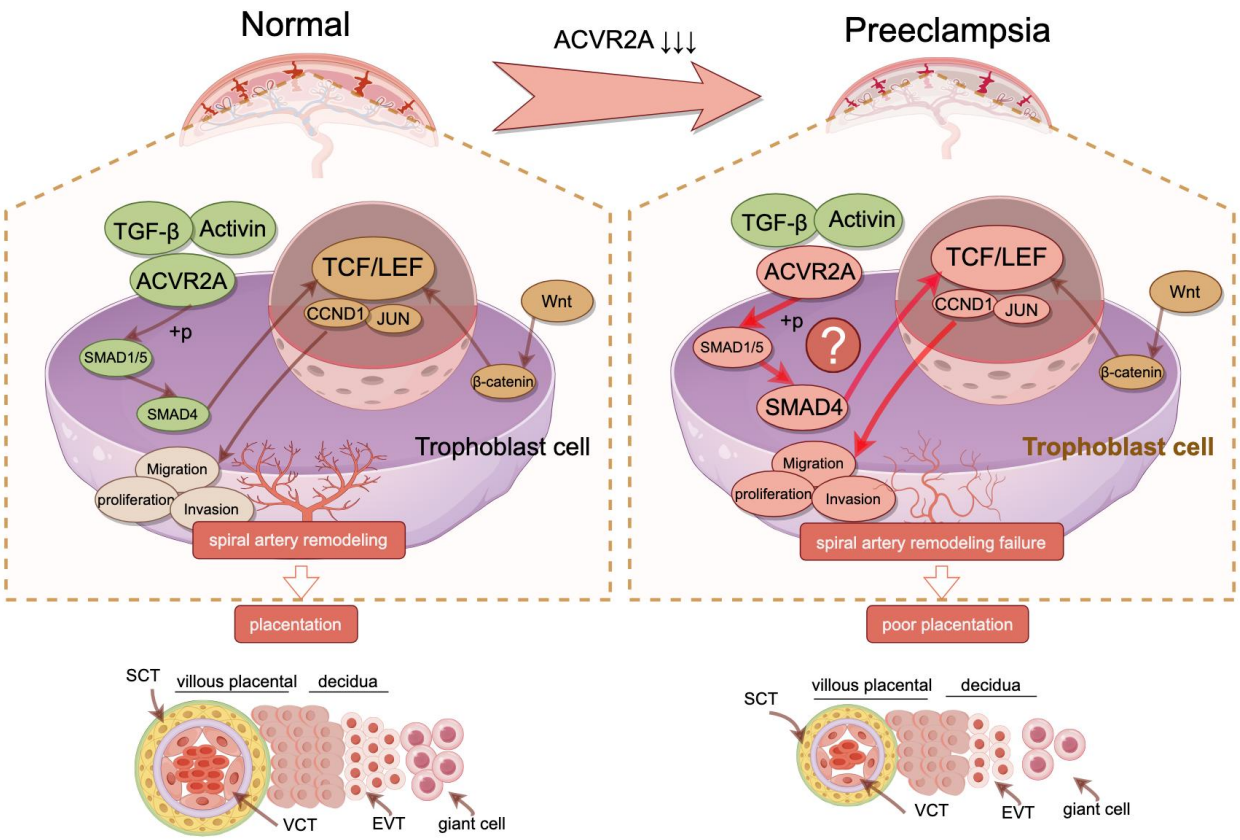

Figure 7 illustrates the inhibitory effect of ACVR2A on trophoblast cell invasion, migration, and proliferation through the TCF7/c-JUN pathway. (Colors: Green: Normal conditions and functional pathways. Red: Abnormalities or disrupted pathways in preeclampsia. Arrows: Solid Dark Brown Arrows: Normal signaling pathways and interactions. Bold Red Arrows: Disrupted or abnormal signaling pathways in preeclampsia.)The typical WNT pathways are intricately connected with TGFβ and ACVR2A. ACVR2A influences TCF7 transcriptional activation via the SMAD1/SMAD5-SMAD4 axis, subsequently impacting genes such as JUN, CCND1, and others, ultimately leading to the regulation of trophoblastic cell invasion, migration, and proliferation (draw by FigDraw).

Figure 6. Validation through RT-PCR and Immunohistochemistry: ACVR2A Modulates Cellular Behavior via the TCF7/c-JUN Pathway.

(A)qRT-PCR analysis of DEGs (Wnt3, Wnt4, TCF7, TCF7L1,CCND1, c-jun) expression enriched in WNT/TCF pathway following HTR8/SVneo ACVR2A knockout.

(B)qRT-PCR analysis of DEGs (Wnt3, Wnt4, TCF7, TCF7L1,CCND1, c-jun) expression enriched in WNT/TCF pathway following JAR ACVR2A knockout.

(C)qRT-PCR analysis of DEGs (Wnt3, Wnt4, TCF7, TCF7L1,CCND1, c-jun) expression enriched in WNT/TCF pathway expression in the placenta of normal control pregnant women (NC) and preeclampsia patients (PE).

(D)Immunohistochemical staining of normal control pregnant women and preeclampsia placentas using rabbit IgG anti-human Wnt3, Wnt4, TCF7L1, TCF7L2,CCND1, c-jun antibody. Sections were counterstained with hematoxylin, and positive cells were quantified using ImageJ software.

Table 1 ACVR2A Gene Polymorphisms and Preeclampsia Risk Summary.

Study participants	Associated SNPs	P-value	OR	Nature of variant (s)	Reference
150 PE cases and 175 controls; Philippine women	rs1014064	0.556	0.8699	intronic	(Amosco et al., 2019)
	rs2161983	0.4717	0.8921	intronic	
	Rs1014064, Age, BMI	0.005		intronic	
443 PE cases and 693 controls; Brazil women; association with early-onset preeclampsia found after grouping in accordance to gestational age at delivery	rs1424954	0.002	1.86	promoter region	(L.C. Ferreira et al., 2015)
	rs1014064	0.004	1.77	intronic	
	rs2161983	0.008	1.70	intronic	
	rs3768687	0.039	1.52	intronic	
176 PE cases, 20 eclampsia and 90 controls; Australian/New Zealand women	rs10497025	0.025		intronic	(Fitzpatrick et al., 2009)
	rs13430086	0.010		3'UTR	
	LF004	0.018		intronic	
	LF013	0.018		intronic	
	LF020	0.018		intronic	
1,139 PE cases and 2,269 controls; Norwegian women	rs1014064	0.0184	0.86	intronic	(Linda T Roten et al., 2009)
	rs17742134	0.0214	1.17	intronic	
	rs1424941	0.0171	1.18	intronic	
	rs2161983	0.0196	0.86	intronic	
	rs3768687	0.0214	0.86	intronic	
	rs3764955	0.0327	0.87	intronic	
121 PE cases and 71 controls; Australian/New Zealand women	rs1424954	0.007		promoter region	(E.K.Moses et al.,2006)
	rs1364658	0.04		intronic	
	rs1895694	0.05		intronic	
140 PE cases and 380 controls; Northern Chinese women	rs1424954	0.013	0.687	promoter region	(Feng Yanan et al.,2020)
	rs1014064	0.016	0.693	intronic	
	rs1128919	0.018	0.536	Synonymous	
	rs3768687	0.019	0.701	intronic	
	rs3764955	0.024	1.784	intronic	
	rs13430086	0.029	0.729	3'UTR	
94 PE cases and 116 controls; Turkish women	rs1128919	0.02	0.44	Synonymous	(Burak Zeybek et al.,2012)
	rs13430086	0.02	0.28	3'UTR	
	rs10497025	0.025	0.010	intronic	